

RESEARCH ARTICLE

Open Access



Regional event-based flood quantile estimation method for large climate projection ensembles

Jiachao Chen^{1*} , Takahiro Sayama², Masafumi Yamada² and Yoshito Sugawara²

Abstract

Emerging large ensemble climate datasets produced by multiple general circulation models and their downscaling products challenge the limits of hydrodynamic models because of the immense data size. To overcome this new challenge and estimate the discharge quantiles corresponding to different return periods at all river sections in an entire region, this study proposes an event-based regional approach that uses a nationwide distributed rainfall–runoff model as well as large climate projection ensembles. This approach addresses the high computational burden associated with continuous simulations and solves the problem of conventional event-based simulations serving only a single outlet of a basin. For our analysis, we extracted 372 annual maximum 48 h rainfall events that cover the entirety of Shikoku Island and its eight major river basins. Peak discharges were estimated using a 150 m resolution rainfall–runoff–inundation model. These discharges were then screened using either the peak-over-threshold (POT) method or block maxima (BM) method, and frequency curves were subsequently constructed and evaluated. The primary reason for the necessity of POT or BM was to avoid interference from extraneous low discharges. The POT-based frequency curves showed good accuracy when using peak discharges in the range of the top 10–50%, and the results remain stable within this threshold range. The BM method, employing block sizes of 2–5 years, can generate relatively accurate frequency curves, but the choice of block size introduces significant variations in results among certain basins. Generally, the accuracy of results based on the POT method surpasses that of the BM method. Considering the accuracy, computational cost, and result stability, the POT method is preferred. The error introduced by the regional approach was acceptable with more than half of the relative root-mean-square errors remaining within 10% and basically all of the results are within 20%. The results of the regional approach exhibited good accuracy across climate scenarios and provided consistent information regarding future flood quantiles. This study serves as the foundation for high-resolution future flood risk assessment.

Keywords Large ensembles, Peak over threshold, Flood frequency analysis, Climate change

*Correspondence:

Jiachao Chen
chen.jiachao.52h@st.kyoto-u.ac.jp

¹ Graduate School of Engineering, Kyoto University, Katsura, Nishikyo-ku,
Kyoto 615-8530, Japan

² Disaster Prevention Research Institute, Kyoto University, Gokasho, Uji,
Kyoto 611-0011, Japan



© The Author(s) 2024. **Open Access** This article is licensed under a Creative Commons Attribution 4.0 International License, which permits use, sharing, adaptation, distribution and reproduction in any medium or format, as long as you give appropriate credit to the original author(s) and the source, provide a link to the Creative Commons licence, and indicate if changes were made. The images or other third party material in this article are included in the article's Creative Commons licence, unless indicated otherwise in a credit line to the material. If material is not included in the article's Creative Commons licence and your intended use is not permitted by statutory regulation or exceeds the permitted use, you will need to obtain permission directly from the copyright holder. To view a copy of this licence, visit <http://creativecommons.org/licenses/by/4.0/>.

1 Introduction

Floods, whose risk is influenced by climate change, have substantial economic and social ramifications (Hirabayashi et al. 2013; Winsemius et al. 2018; Tellman et al. 2021). Flood intensity and frequency have been reported to increase due to climate change (IPCC 2021). These changes necessitate proactive risk-management strategies for human settlements, urban planning, and socio-economic development.

Typical flood hazard assessments rely on extensive data collection, detailed hydraulic engineering surveys, and hydrological and hydrodynamic modeling (Martínez et al. 2018; Zeng et al. 2022). Such approaches (e.g. Institute of Hydrology 1999) often adopt statistical methods, such as intensity–duration–frequency or depth–area–duration methods, to design rainfall intensity for a specified return period (Gellens 2002; Sun et al. 2019) and rainfall pattern (Yan et al. 2020). However, because of the variability in precipitation, the impact to different river sections of an event is different, while statistical method selects events by specifying an outlet first, which means the simulation result cannot be used for investigating other river sections in the same basin (e.g., precipitation events that cause a 100-year flood in a particular basin may not necessarily result in floods with the same return period in its sub-basins). Moreover, preparing designed rainfall and conducting hydrologic simulations for all river sections, including sub-basins, over a large region is impractical (Packman and Kidd 1980; Watt and Marsalek 2013). Another issue is that the return period of rainfall and floods has no unified correspondence; thus, results obtained from the design storm may not represent the actual river flood intensities for the return periods (Breinl et al. 2021).

To achieve reliable national- or global-scale flood risk assessment, several approaches have been proposed, including analysis-based and cascade modeling approaches (Dottori et al. 2016; Hoch and Trigg 2019). The analysis-based modeling approach utilizes regional flood frequency analysis (FFA) with observed discharge datasets to estimate peak discharge and employs cluster algorithms to extend the results to ungauged basins based on catchment descriptors (Sampson et al. 2015; Smith et al. 2015; Wing et al. 2017, 2021). The cascade modeling approach, exemplified by the utilizations of GloFAS (Dottori et al. 2016), GLOFRIS (Winsemius et al. 2013), and ECMWF (Pappenberger et al. 2012), typically employs a land surface model with a river routing model such as CaMa-Flood (Yamazaki et al. 2013) or LISFLOOD (Bates et al. 2010) to compute flood peaks over large domains based on long-term simulations. The simulated flood peak discharges at each river section can then be statistically analyzed to compute those with certain frequencies. The estimated discharges are used

as inputs to high-resolution hydrodynamic models. For example, Alfieri et al. (2014) employed LISFLOOD to generate a continuous 21-year daily discharge sequence for the pan-European region at a resolution of 5 km and mapped flood hazards at a resolution of 100 m. However, these approaches have difficulties in handling large climate projection ensembles. The analysis-based modeling approach relies on an observed discharge dataset, which is unavailable for future scenarios. Thus, the cascade modeling approach is more applicable for climate change impact assessment. Nevertheless, even with low-resolution cascade simulations, the computational requirements are significant because of the numerous climate projection ensembles spanning several decades. Moreover, errors and uncertainties are associated with discharge results from simulations at low resolutions (Meade et al. 1991; Alfieri et al. 2014; Zhao et al. 2017). Sampson et al. (2015) suggested that its applicability in regions with low-quality topographic data is yet to be demonstrated and quantified. Therefore, considering new approaches for large-scale flood simulations under climate change and obtaining accurate peak discharges at specific return periods for local flood hazard mapping are necessary.

In this study, we propose an event-based approach to obtain the peak discharge in all river sections. To distinguish this approach from the conventional event-based approach (called the basin approach in this study), which focuses only on a single-basin outlet, the new approach is hereafter referred to as the regional approach. The regional approach aims to reduce the computational burden with relatively low errors for large climate projection ensembles.

Event-based simulations, including the regional approach, confront the challenge of precipitation variability. Some events lead to high discharge in specific river sections and low discharge in others. These cases ultimately result in severe errors in the FFA. To reduce these impacts and obtain accurate peak discharges for each river section at specific return periods, we further examine screening methods using block maxima (BM) and peak over threshold (POT). The problems addressed in this study are as follows:

1. Which method—BM or POT—is more suitable for frequency analysis based on the result using regional approach? How should its corresponding parameters be selected?
2. How much error will be introduced by the regional approach?
3. Will the approach be valid under future climate conditions?

Based on the challenges faced when studying floods under climate change, this study provides a novel approach for large-scale and high-resolution flood simulations. Additionally, the cases selected in this study shed light on the potential magnitude of errors and uncertainties introduced by the regional approach, which can inform efforts for further improvement.

2 Methods

2.1 Regional approach

Figure 1 compares the key steps of the conventional basin approach and the proposed regional approach. Both approaches extract extreme rainfall events. While the basin approach extracts events based on basin average precipitation, the regional approach extracts them based on an entire region, in this case Shikoku Island, which contains multiple river basins. The former approach has been adopted in Japan for estimating annual maximum peak discharges corresponding to different return periods (i.e., flood quantiles) by simulating flood discharges with a rainfall–runoff model. In case we use a distributed rainfall–runoff model, we can simulate discharges even at tributaries within the basin. However, the estimated discharges do not necessarily represent the quantiles at each river section, except for the outlet of the basin, because of the spatial variability of precipitation of the extracted events. In order to obtain a flood quantile map, which is our objective here, we have to apply the basin approach for each river sections even within a river basin. Obviously, that requires enormous computation, which is not practically possible. As an alternative approach, we introduce the regional approach. The method extracts large number of rainfall events from a climate projection ensemble based on the amount of rainfall over a region. Then, we estimate flood peak discharges using a distributed rainfall–runoff model. Here we hypothesize that discharges with longer return periods at different river sections have high probability to be affected by a series of extreme precipitation events. That means if we extract sufficient number of events and adequately screen the peak discharge data based on POT or BM, we can estimate the flood quantiles at all river sections. To evaluate the accuracy, we can compare the one estimated by the basin approach (at the outlet) and the regional approach. Given the ample data provided by climate projection ensembles spanning centuries, the criterion for extreme events in this study was the annual maximum 48 h precipitation (48 h-AMS). Subsequently, a distributed high-resolution hydrologic model, the rainfall–runoff–inundation (RRI) model, was employed to simulate the discharges for each river section. Because of the variability in precipitation, event-based simulation results may contain low discharges, which necessitate the adoption of

the POT and BM methods as potential solutions for estimating the frequency curves. The flood quantiles were obtained by further screening the discharge and conducting FFA.

In this study, discharges from the basin outlets derived via the basin approach were considered as references. The criterion for extreme events in the basin approach remains the 48 h-AMS and computed for each basin within the study area. A comparison was made between the results obtained from the basin and regional approaches.

A numerical experiment was conducted on Shikoku Island (applying the regional approach) and its eight major river basins (applying the basin approach as a reference). In particular, we evaluated the performance of the regional approach with different screening parameters. For the POT method, the screening parameter is a threshold above which they will be included in the frequency analysis. For the BM method, the screening parameter is an interval at which the maximum value is determined, referred to as block size (Zou et al. 2021). In addition, we verified the performance of the regional approach in the 2 K and 4 K scenarios (the Sea Surface Temperature (SST) rises 2 K and 4 K, respectively) by comparing the flood quantiles with those from the basin approach. The effects of the frequency analysis method and sources of error are discussed later in this paper.

2.2 RRI model

This study used the RRI model, a two-dimensional distributed hydrodynamic model, to simulate the physical processes involved in the transition from precipitation to runoff (Sayama et al. 2012). It discretizes the study area and divides it into land and river channel grids using two-dimensional and one-dimensional diffusion wave equations to describe water movement, respectively. River channel grids contain information of levees, allowing the RRI model to simulate runoff overflows and returns in the river grids. In terms of runoff components, the RRI model considers surface and lateral subsurface flows, which are important in mountainous areas (Sayama and McDonnell 2009). The Green–Ampt model (Green and Ampt 1911) was used to model infiltration. The fifth-order Runge–Kutta formula (Cash and Karp 1990) was used as the numerical scheme to ensure efficiency and accuracy. The RRI model performs well in Japan and Southeast Asian countries (Sayama et al. 2015, 2017, 2020; Bhagabati and Kawasaki 2017; Yamamoto et al. 2021; Try et al. 2022). Due to the good performance, Rasmy et al. (2019) further developed a Water and Energy Budget-based RRI (WEB-RRI) model in Sri Lanka for local water resources and disaster management under a changing climate. Even though the WEB-RRI model is advantageous in terms of estimating long-term water and energy

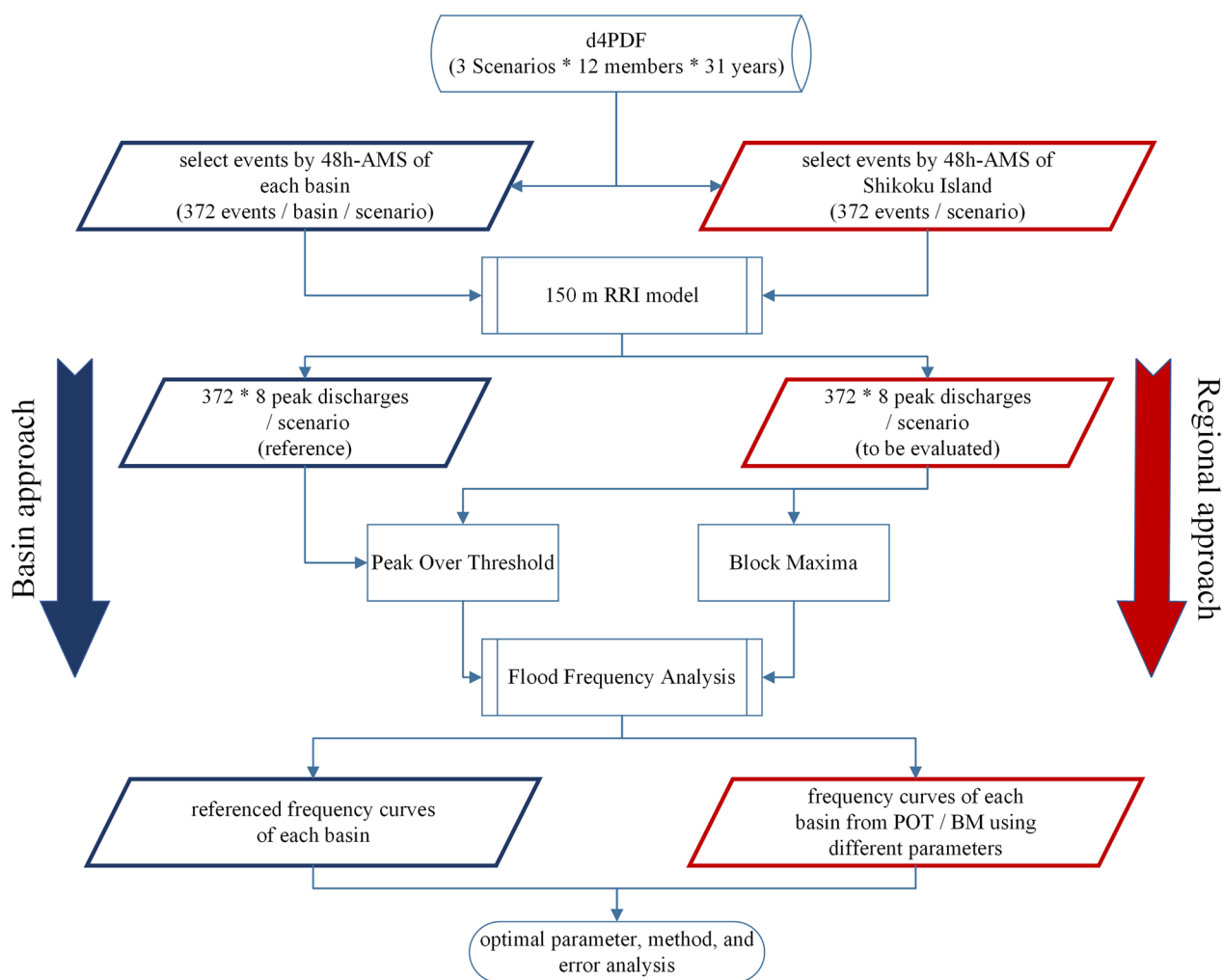


Fig. 1 Flow chart of the basin and regional approaches for this study

budget, which is essential for the applications of the model to water resources management, the original RRI model is thought to be suitable for the present study because of the physically sound and simple representations of the subsurface and surface runoff processes, essential for event-based storm runoff predictions even in ungauged basins. In a previous study, the RRI model had been well calibrated across Japan, and these model parameters were followed in this study (Yamada et al. 2022; Yamakita 2023).

The peaks of the RRI model results based on the 48 h-AMS extracted for each basin are called the basin annual maximum flood series (AMFS), which was used as the reference for this study and has a total of 372 (discharge peaks) × 8 (basins) × 3 (scenarios) values. The simulation results using 48 h-AMS, which were extracted for Shikoku Island and then extracted at the outlet of each basin, are called the regional AMFS, which also has 372 × 8 × 3 values.

2.3 Frequency analysis method

Depending on the sample selection method, frequency analysis can be classified into the BM and POT methods (Mostofi Zadeh et al. 2019). The BM method divides a time series into equal-sized blocks and extracts the maximum value for each block. The most typical application of the BM method in hydrology is the annual maximum method. The L-moment method is used to estimate parameters of each distribution (Hosking and Wallis 1993). For the BM method, the optimal distribution is ultimately determined to be the Pearson Type III (PE3), as given by Eq. 1, among those tested distributions including generalized logistic (GLO), generalized extreme value (GEV), generalized normal (GNO), generalized Pareto distribution (GPD) and PE3. The results of the goodness-of-fit statistic Z, used for selecting the optimal distribution, are detailed in Additional file 1: Tables S1–S3. However, according

to the definition of block maxima, only one value can be selected within a block. That means, in years with abundant precipitation, multiple flood events may occur, but the second-largest discharge cannot be chosen as an “extreme value”, even if it surpasses the maximum in a drought year. While in a drought year, no matter how low the discharge was, it will be selected as an “extreme value”. Due to the above-mentioned limitation, the BM method is possible to miss high values and select low values, causing inaccurate frequency analysis results (Ferreira and de Haan 2015). The POT method selects all data above a certain threshold. The newly created sequence theoretically follows the GPD (Eq. 2) (Lang et al. 1999).

$$PE3(x) = \frac{\sigma^\xi}{\Gamma(\xi)}(x - \mu)^{\xi-1} \exp(-\sigma(x - \mu)) \quad (1)$$

$$GPD(x) = \begin{cases} 1 - (1 + \xi(\frac{x-\mu}{\sigma}))^{-1/\xi} & \text{for } \xi \neq 0 \\ 1 - \exp(-\frac{x-\mu}{\sigma}) & \text{for } \xi = 0 \end{cases} \quad (2)$$

where ξ , μ , and σ are the shape, location, and scale parameter, respectively. All three parameters are estimated by L-moment method. The block size and threshold are the key parameters that must be artificially determined for the BM and POT, respectively. Although many studies have been conducted on the choice of a reasonable threshold for a POT, the aim is to find a low threshold for using as much data as possible (Langousis et al. 2016; Mostofi Zadeh et al. 2019; Swetapadma and Ojha 2021). In this study, because of the numerous climate projection ensembles, we attempted to use high thresholds to balance efficiency and accuracy. Due to the spatial variability of precipitation, some of the regional 48 h-AMS may result in low discharges in specific sub-basins. Therefore, using a high threshold is advantageous for filtering low discharges. Furthermore, because the POT method allows for more precise threshold control, it was chosen as the frequency analysis method for the basin AMFS. As the design floods of most infrastructures focus on a return period longer than 10 years, the maximum threshold for the POT was set to the top 10% of the AMFS in descending order. Correspondingly, the maximum block size of the BM was set to 10 years. A series of possible

parameters, categorized as Model 1–6, are listed in Table 1. The extracted AMFS were nonstandard annual series, the probability P corresponding to the standard return period T must be calculated using Eq. 3, where the $np\gamma$ refers to the number of discharge peaks per year.

$$P = 1 - \frac{1}{T \times np\gamma} \quad (3)$$

The FFA results were evaluated using the relative bias (BIAS; Eq. 4) and relative root-mean-square error (RRMSE; Eq. 5).

$$BIAS = \frac{y_e - y_r}{y_r} \times 100\% \quad (4)$$

$$RRMSE = \frac{\sqrt{\frac{1}{n} \sum (y_{e*} - y_{r*})^2}}{\frac{1}{n} \sum y_{r*}} \quad (5)$$

where y_e and y_r are the quantiles corresponding to different return periods between 10 and 1000 years every 1 year. They are estimated based on the fitted curves to the simulated peak discharges by the regional and the basin approaches, respectively. The BIAS indicates how the regional approach is biased compared to the basin one. On the other hand, RRMSE compares the simulated peak discharges by the basin approach (y_{r*}) and the fitted curve by the regional approach denoted as y_{e*} , which are corresponding to discrete return periods. Hence unlike the BIAS index, the RRMSE indicates the degree of errors more directly by the regional approach compared to the reference one without uncertainty associated to the curve fitting to the y_{r*} . The model results can be regarded as excellent if $RRMSE \leq 10\%$, good if $10\% < RRMSE \leq 20\%$, fair if $20\% < RRMSE \leq 30\%$, and poor if $RRMSE > 30\%$ (dos Santos et al. 2016).

3 Study area and data

3.1 Study area

The study area of Shikoku Island, Japan, is located between 132–135° E and 32.5–34.55° N (Fig. 2). It is a relatively independent area separated from Honshu Island by the Seto Inland Sea to the north and surrounded by the Pacific Ocean on its three other sides. The area of Shikoku Island is 18,785 km², 70% of which is covered by

Table 1 Parameters of the POT and BM data selection methods

| Models | 1 | 2 | 3 | 4 | 5 | 6 |
|-----------------|----------|---------|---------|---------|---------|---------|
| POT (threshold) | 10% | 20% | 30% | 40% | 50% | 100% |
| BM (block size) | 10 Years | 5 Years | 4 Years | 3 Years | 2 Years | 1 Years |

forests. Similar to other regions of Japan, it is mountainous and steep, with the highest peak on the island (with a summit of 2000 m) descending to sea level within 50 km.

Shikoku Island has an average annual temperature of nearly 14 °C, making it a major producer of early rice crops in Japan (Yoshida et al. 2012). The spatial distribution of average annual precipitation varies considerably due to frontal storms and typhoons (Kamahori and Arakawa 2018; Tada et al. 2018; Otaki et al. 2022), from about 1200 mm in the north to 2500 mm in the south and 4000 mm in the mountains (Yao and Creed 2005).

The main reasons for selecting Shikoku Island as the study area were its relatively independent geographical conditions, significant differences in precipitation, and flood-prone terrain. The morphological parameters of its eight major river basins are listed in Table 2.

3.2 Data

The database for Policy Decision-making for Future climate change (d4PDF) is an open-access dataset used to study climate change impacts and plan adaptation (Mizuta et al. 2017). The dataset was dynamically downscaled from the 60 km Meteorological Research Institute Atmospheric General Circulation Model 3.2 (MRI-AGCM 3.2), using a 20 km Non-Hydrostatic Regional Climate Model (NHRCM) (Sasaki et al. 2011). External forcing was derived from MRI-AGCM 3.2 and the boundary conditions were derived from MRI-CM (Deushi and Shibata 2011) and MRI-CGCM3 (Yukimoto et al. 2012). The differences between simulations in the same scenario were mainly caused by the difference in SST between current and future climate (Δ SST) and perturbations (δ SST). The spatiotemporal distributions

Table 2 Morphological parameters of the eight major river basins of Shikoku Island

| Basin | Area (km ²) | Length (km) | Elevation of river source (m) |
|-----------|-------------------------|-------------|-------------------------------|
| Yoshino | 3750 | 194 | 1897 |
| Watari | 2186 | 196 | 1336 |
| Niyodo | 1560 | 124 | 1982 |
| Hiji | 1210 | 103 | 460 |
| Naka | 874 | 125 | 1929 |
| Monobe | 508 | 71 | 1770 |
| Shigenobu | 445 | 36 | 1233 |
| Doki | 140 | 33 | 1059 |

of Δ SST were provided by six CMIP5 (Coupled Model Intercomparison Project phase 5) models (Mizuta et al. 2017). Owing to the large number of ensembles that facilitate uncertainty reduction and good extreme event reproducibility (Tanaka et al. 2018; Ishii and Mori 2020), d4PDF has been widely used to study extreme precipitation, snowfall, drought, and water resource assessment (Kawase et al. 2016, 2020; Ohba and Sugimoto 2019; Hattuzuka et al. 2020; Miyasaka et al. 2020; Ohba et al. 2022).

The data used in this study were further downscaled using the 5 km NHRCM. This dataset is called dynamical downscaling data for near-future atmospheric projection (from Tohoku to Kyushu) by the Social Implementation program on Climate change Adaptation Technology (SI-CAT DDS5TK), which is funded by the Ministry of Education, Culture, Sports, Science and Technology, and covers the Tohoku to Kyushu regions of Japan. This included three scenarios (current, 2 K Δ SST, and 4 K Δ SST) with 31 years \times 12 members (2 \times 6 SST patterns) (Mizuta et al. 2017; Fujita et al. 2019). More specific parameter settings can be found in Sasai et al. (2019). These 12 members were used as a complete dataset.

4 Results

4.1 Evaluation of the current scenario

A primary objective of this study was to determine the optimal combination of frequency analysis methods for integration into the regional approach. Figure 3, using the Watari river basin as an example, illustrates the frequency curves fitted by the POT and BM methods using the six parameters from Table 1. It is crucial to note that different parameters can result in varying data samples, causing the *x*-axis's starting position to be less than 10 years. However, since this study primarily focuses on fitting beyond a 10-year return period, the calculation of RRMSE and the display of fitting results only use results

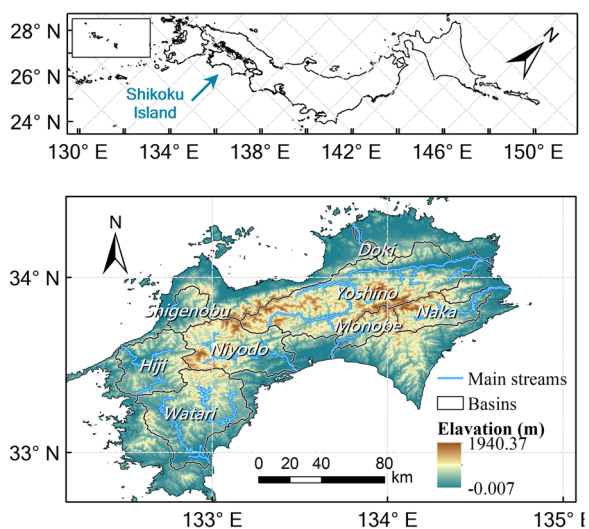


Fig. 2 Overview of Shikoku Island

exceeding 10-year return period. The RRMSE in the figure calculates the error between the predictions of the regional approach and the basin AMFS, and used for assessing the accuracy of the regional approach-based frequency curve. According to the RRMSE, models 1–5 using the POT method in the Watari Basin (i.e., employing the top 10–50% of basin AMFS as the threshold) yield stable and satisfactory results.

To obtain robust conclusions, we examined the results for eight major basins across Shikoku Island, and their RRMSE is summarized in Fig. 4. The blue histograms represent RRMSE based on the POT method, the orange histograms represent RRMSE based on the BM method, and the grey line reflects the error of the fitted curve under reference conditions (i.e., the RRMSE from basin approach). The reference RRMSEs demonstrate excellent goodness of fit of the basin approach, which indicates the capacity of being reference, with values consistently below 10%, meeting the criteria for excellence. Overall, the POT method appears to offer higher accuracy. Specifically, models 1–5, corresponding to the use of the top 10–50% of regional AMFS, demonstrate high accuracy across basins. Their results show no significant difference in magnitude from the reference RRMSE (i.e., the grey line). Model 6, which utilizes 100% of the regional AMFS, tends to yield inferior results. As analyzed in the issue of the limitations of event-based simulations, the simulation results of event set in some river sections may include extremely low discharges, which is caused by precipitation variability, and thereby influence the fitting of the frequency curve. This further underscores the necessity of employing high thresholds to prevent these “non-extreme” data from frequency analysis.

For the BM method, models 1 and 6 (corresponding to block sizes of 10 years and 1 year, respectively) typically exhibit the poorest performance. The results of models 2–5 vary by basin, making it challenging to determine the optimal block size or provide a recommended range. This variability is attributed to the inability of the BM sampling method to effectively exclude “non-extreme” discharges. Additionally, the order of occurrence of peak discharges influences the sampling results, introducing considerable uncertainty. Therefore, considering the accuracy and the robust of threshold, the POT method is recommended.

Figure 5 shows the POT-based frequency curves for the current scenario with threshold of 10%. According to the RRMSE values, all the regional results have a good fit. The distribution of data points in Fig. 5 shows that most of the regional AMFS and basin AMFS overlap or have small differences, especially for extreme discharges with long return periods, which confirms our hypothesis that

most of the peak discharges in different river sections originate from different events, but ultimately from an extreme event group.

The Monobe River Basin presents a unique case, showing a poor overlap of discharge with long return periods and a large error in the maximum value. By manual checking, we found that the maximum values of the basin AMFS and regional AMFS originated from two different precipitation events. This suggests that the maximum value of the basin AMFS originated from a local extreme precipitation event. Due to the spatial variability of precipitation, it was missed in the search for extreme precipitation across the entire region. The maximum value of the regional AMFS corresponded to the second-largest value of the basin AMFS. Similar mismatches were observed in the subsequent AMFS in the Monobe River Basin. Theoretically, the longer the return period of discharges, the greater the FFA model error caused by the mismatch. This indicates that the regional approach can be further improved by determining new extraction approaches that can identify these crucial local extreme precipitation events or alternative frequency analysis methods that can reduce the sensitivity to ranking.

A relatively high BIAS was observed in the Doki river basin, which has the smallest area among the eight basins, consequently having low discharge in most years. However, because of their topography and morphology, they are more sensitive to precipitation, which leads to an extremely high discharge from the largest precipitation event, and therefore, the frequency curve fails to fit discharge with return period longer than 100 years.

Overall, the BIAS varied between $\pm 10\%$ for different return periods and the interval of BIAS variation was limited to 0 to -5% in some basins. The regional approach mitigates but does not entirely eliminate the influence of precipitation variability.

4.2 Evaluation on future scenarios

In the 2 K and 4 K warming scenarios, the POT method with the top 10% AMFS yielded good outcomes. The RRMSEs of each basin when employing the top 10% AMFS are summarized in Table 3. In the current scenario, five basins were rated as excellent, whereas three basins received good ratings, consistent with the results presented in Fig. 5. In the 2 K warming scenario, four basins were rated excellent, two good, and two fair. In the 4 K warming scenario, five basins achieved excellent ratings, and three received good ratings. Notably, none of the basins were rated as poor in any of the three scenarios. Hence, we concluded that the constructed quantile estimation model performs well and is stable across the three scenarios.

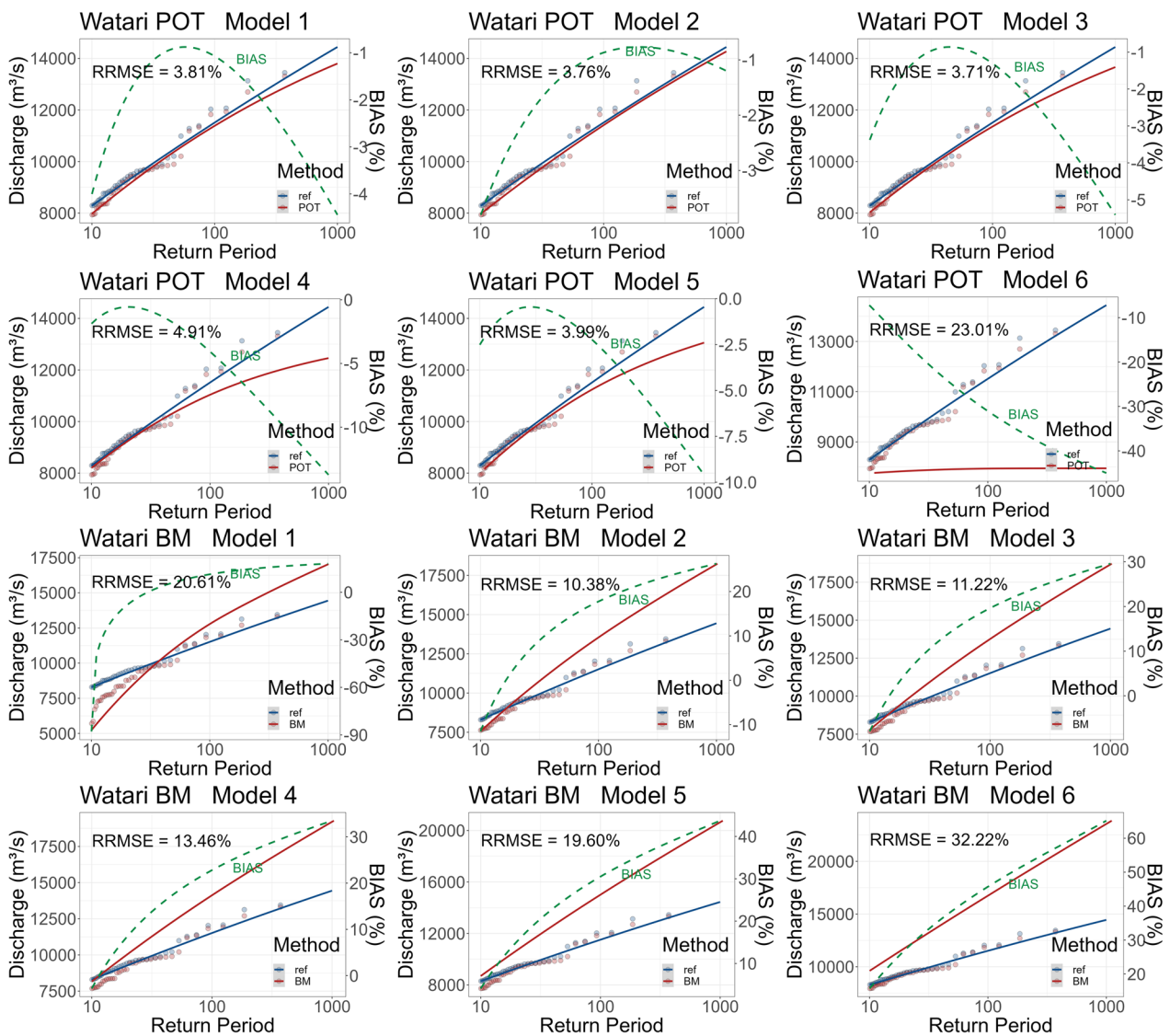


Fig. 3 Accuracy comparison of applying the POT and BM methods using different parameters for Watari basin. Model 1–6 indicate the precipitation data come from current scenario and the parameter corresponds to the value of Model 1–6 in Table 1. Blue points and lines represent the basin AMFS and frequency curve, respectively. Red points and lines indicate the regional AMFS and frequency curve, respectively. Green dashed lines show the BIAS between the basin and regional results

Figure 6 shows the estimation results of the discharge quantiles for each basin with the POT method and 10% AMFS in the 2 K warming scenario. In this scenario, we observed a general underestimation in discharges from regional approach. Manual checking revealed that these discharges originated from the same precipitation event, with peak times differing by several hours. This situation arose mainly because the precipitation only extracted for 48 h, whereas some extreme events lasted longer than 48 h and exhibited variations in peak times among the different basins. Consequently, in some basins, precipitation input ceased before the true peak was reached.

Climate change affects the characteristics and durations of extreme precipitation events. Therefore, in the future, event extraction schemes that do not depend on fixed durations must be considered. Overall, BIAS varied between $\pm 20\%$ and within $\pm 10\%$ in some basins.

Figure 7 shows the estimation results of the discharge quantiles for each basin using the POT method and 10% AMFS under the 4 K warming scenario. In this scenario, large RRMSE values were observed in the Yoshino and Doki basins. From the perspective of precipitation events, the maximum 48 h-AMS in the Yoshino basin, whether extracted by the basin approach or the regional

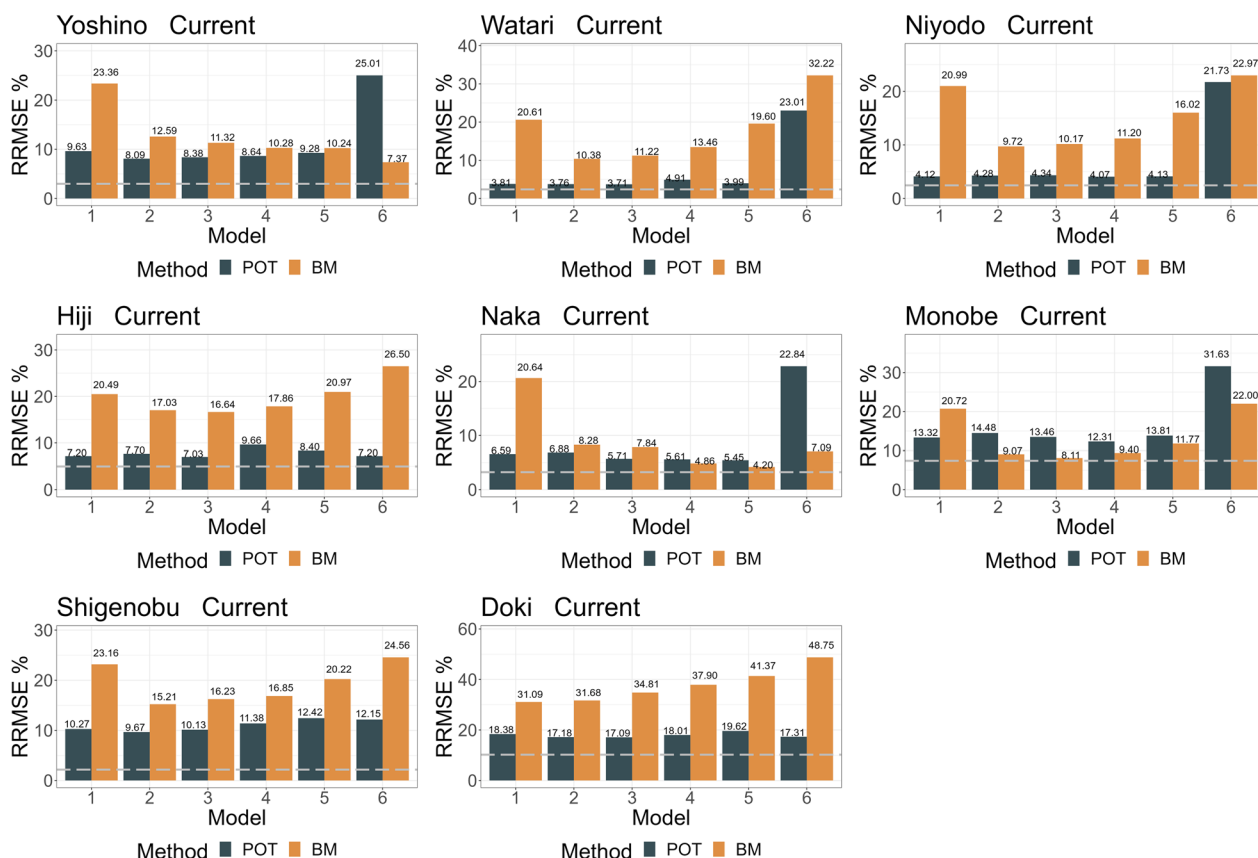


Fig. 4 RRMSEs of the eight basins using different methods and parameters under the current scenario. The grey dash line represents the RRMSE between the predictions of the basin approach and the basin AMFS

approach, is associated with the same precipitation event. However, due to the actual precipitation process exceeding 48 h and the event selection method being set with a 48 h time window, the start times of the basin 48 h-AMS and the regional 48 h-AMS differ by 4 h. During this time, the precipitation center shifts from the Yoshino basin to another basin, resulting in a significant reduction in the discharge calculated by the regional method, ranking it 30th instead of the first. This further underscores the need to develop an event extraction method with non-fixed durations in future studies. In the Doki Basin, the frequency curves fit well with the corresponding points, indicating that the GPD distribution is capable to fit the extreme discharges. While due to the limitation on precipitation extraction method, there is a significant difference between the regional AMFS and basin AMFS, leading to large error.

Overall, increasing the threshold for the FFA can effectively improve the accuracy of the results by excluding low discharges. 10–50% of the AMFS were found to be reasonable threshold. Considering the accuracy and result stability, the POT method is the preferred

frequency analysis method. The spatiotemporal variability of precipitation remains the primary source of error, and its impact may become more pronounced with climate change. However, this impact is expected to be mitigated in the future by improving precipitation event extraction methods. In summary, the regional approach yielded relatively accurate flood quantiles for each basin at a relatively low computational cost.

5 Discussion

This study proposes a regional approach to estimate the flood quantiles of all river sections from finite extreme precipitation events. This approach is expected to be valid under diverse climatic conditions. In the regional approach framework, a crucial step is aimed at further screening discharges, offering two alternatives: POT and BM. “Which option, accompanied by what parameters, proves optimal? What is the magnitude of the error and how does it perform in future scenarios?” These three fundamental questions have become the focal points of this study.

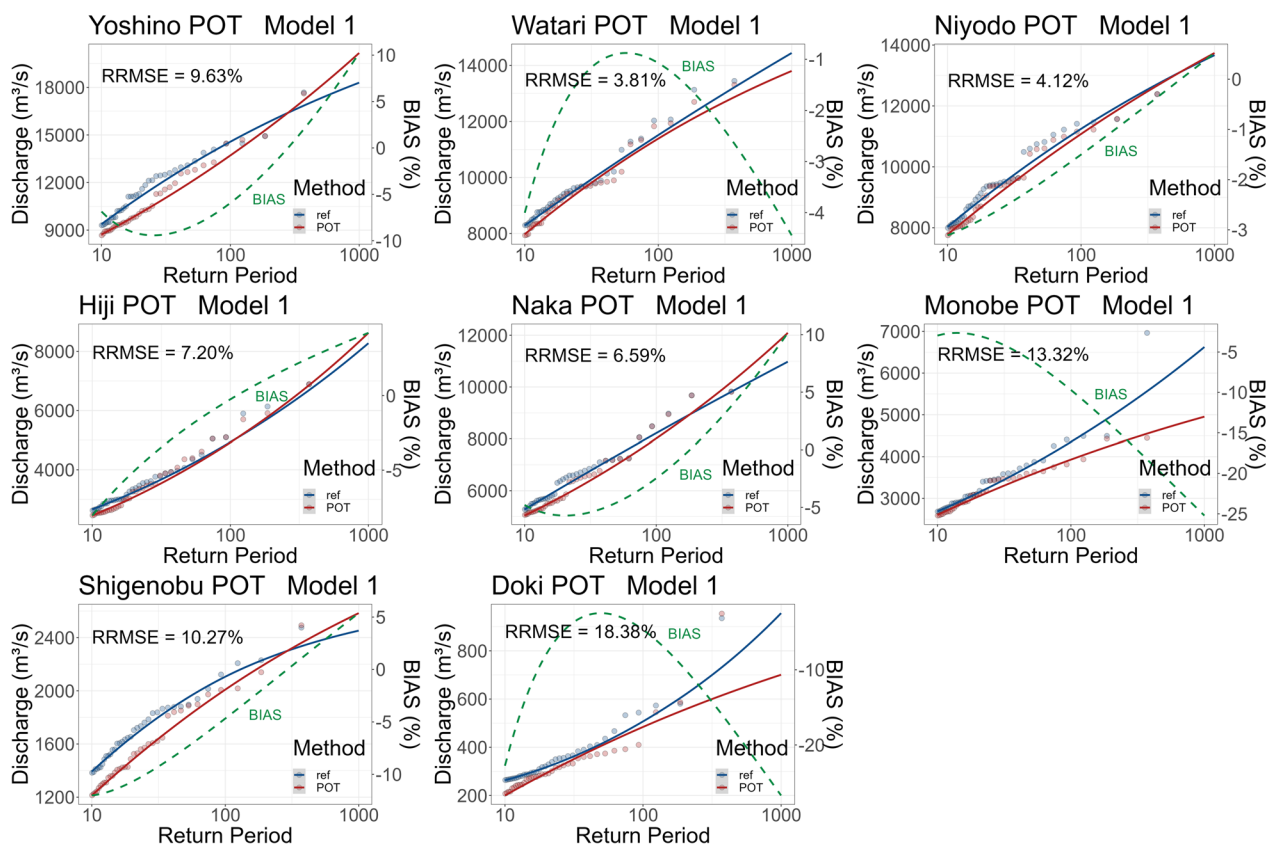


Fig. 5 Estimation results of discharge quantiles for different basins using the POT methods with the top 10% AMFS. The meaning of elements in the figure can refer to Fig. 3

Table 3 Performance of regional results in different scenarios

| Scenarios | Excellent (RRMSE ≤ 10%) | Good (10 < RRMSE ≤ 20%) | Fair (20% < RRMSE ≤ 30%) | Poor (RRMSE > 30%) |
|-----------|----------------------------|----------------------------|-----------------------------|-----------------------|
| Current | 5 | 3 | 0 | 0 |
| 2 K | 4 | 2 | 2 | 0 |
| 4 K | 5 | 3 | 0 | 0 |

The initial purpose of the POT method was to avoid missing high discharges during rainy years, which likely occurs when employing the BM method. To perform a more reliable FFA, the POT method typically sets a relatively low threshold to maximize the data utilization. This study sets a high threshold mainly based on two considerations. Firstly, it aims to eliminate the influence of low values at short return periods, ensuring a robust fit for extreme values at long return periods. Secondly, the availability of multi-year data from climate ensembles, such as the 372 years of precipitation data provided by SI-CAT DDS5TK in this study, allows for the construction of reliable FFA even when employing a

higher threshold. Hence, a relatively high threshold value was established. Notably, the selection of the threshold constitutes a highly technical task within the POT method as it affects data independence, distribution assumptions, and sample size (Lang et al. 1999; Beguería 2005). Previous studies have predominantly focused on threshold selection (Langousis et al. 2016; Swetapadma and Ojha 2021). Nevertheless, the demand arises from attempts to employ a low threshold instead of a high threshold. This is because the lower threshold limit (more than once per year) for satisfying the GPD is ambiguous, whereas it is tenable if the threshold is adequately high. Independence was guaranteed because

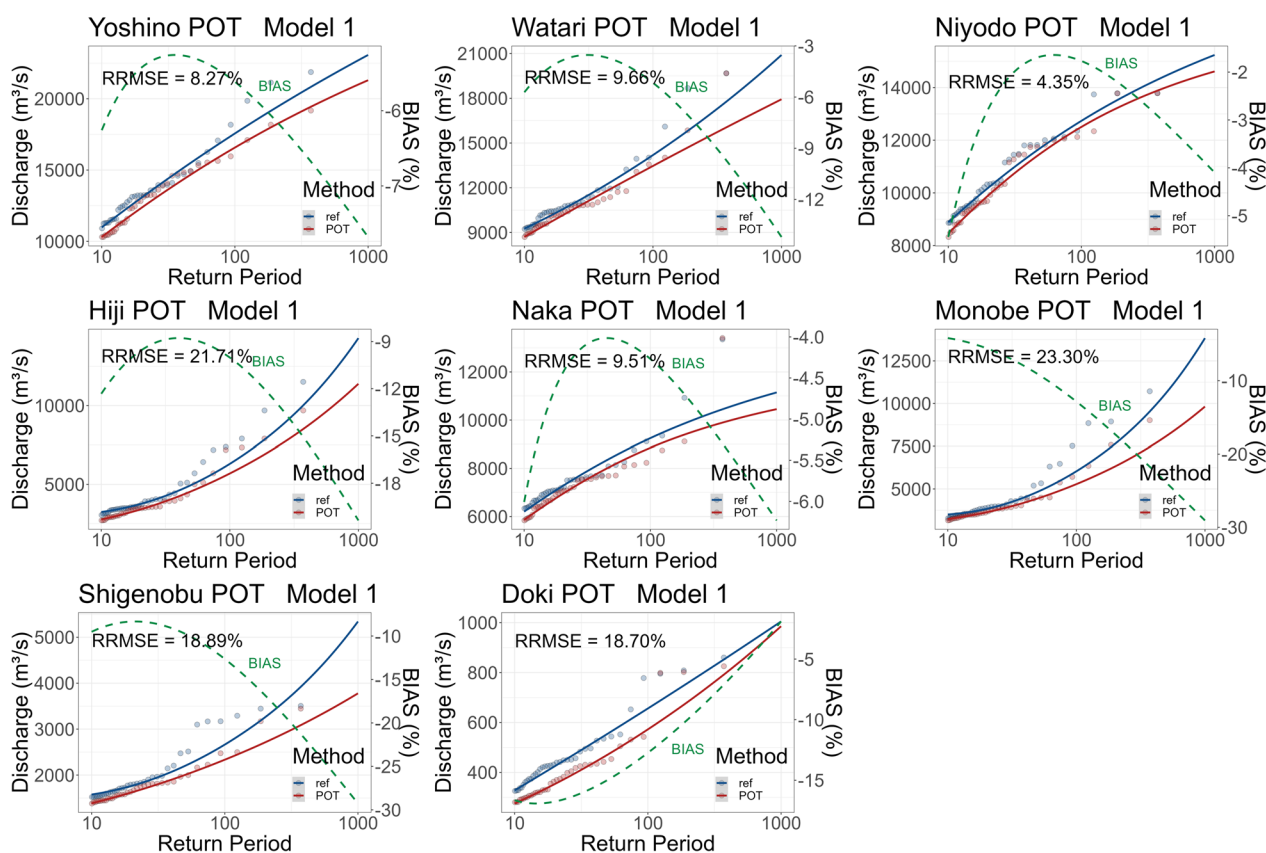


Fig. 6 Estimation results of discharge quantiles for different basins using the POT methods with the top 10% AMFS for the 2 K warming scenario

the discharges were from different precipitation events, and a large ensemble ensured the data size.

The POT and BM methods have two primary distinctions: sampling technique and assumed distribution. The divergent outcomes of the sampling techniques are shown in Fig. 8. After the screening process, the BM method still retained discharges close to zero in certain basins, such as Watari, Hiji, Shigenobu, and Doki. However, the POT method does not encounter this issue. Due to its inability to entirely eliminate periodic fluctuations that may exist in the data (e.g., missing several flood peaks in wet years and including low discharges in dry years as extremes), the BM method may not be suitable for filtering low discharges using the regional approach. This limitation introduces uncertainty into the results. Low discharges play a more significant role in estimating the distribution curve parameters because they constitute a substantial proportion of the extremes. Consequently, greater emphasis is placed on fitting short return periods, whereas the accuracy of long return period predictions, which hold greater importance for decision-makers, is disregarded. Theoretically, the GPD exhibits better adaptability to heavy-tailed distributions (Madsen et al. 1997).

Cunnane (1973) demonstrated that POT performed better when the average annual occurrence was higher than 1.6, and a similar conclusion was derived in other studies (Madsen et al. 1997; Bezak et al. 2014). According to the results of this study, the POT method exhibits excellent robustness and accuracy, making it a superior choice for integration into the regional approach.

Errors in the quantile estimations can be classified into two types. The first type comes from the gap between the sample data and population distribution, which is unavoidable. This type of error can be considered as the goodness of fit of the results from the basin approach (Fig. 3) when the basin approach is regarded as a reference. Generally, the first type of error accounted for over half of the total errors. The second type of error stems from the differences in discharge when employing a regional approach, which mainly caused by the precipitation variability.

The accuracy of the results provided two important insights. First, despite recent research indicating that storm temporal patterns under climate change will become more acute and have shorter durations (Wasko et al. 2021), the regional approach remains valid under

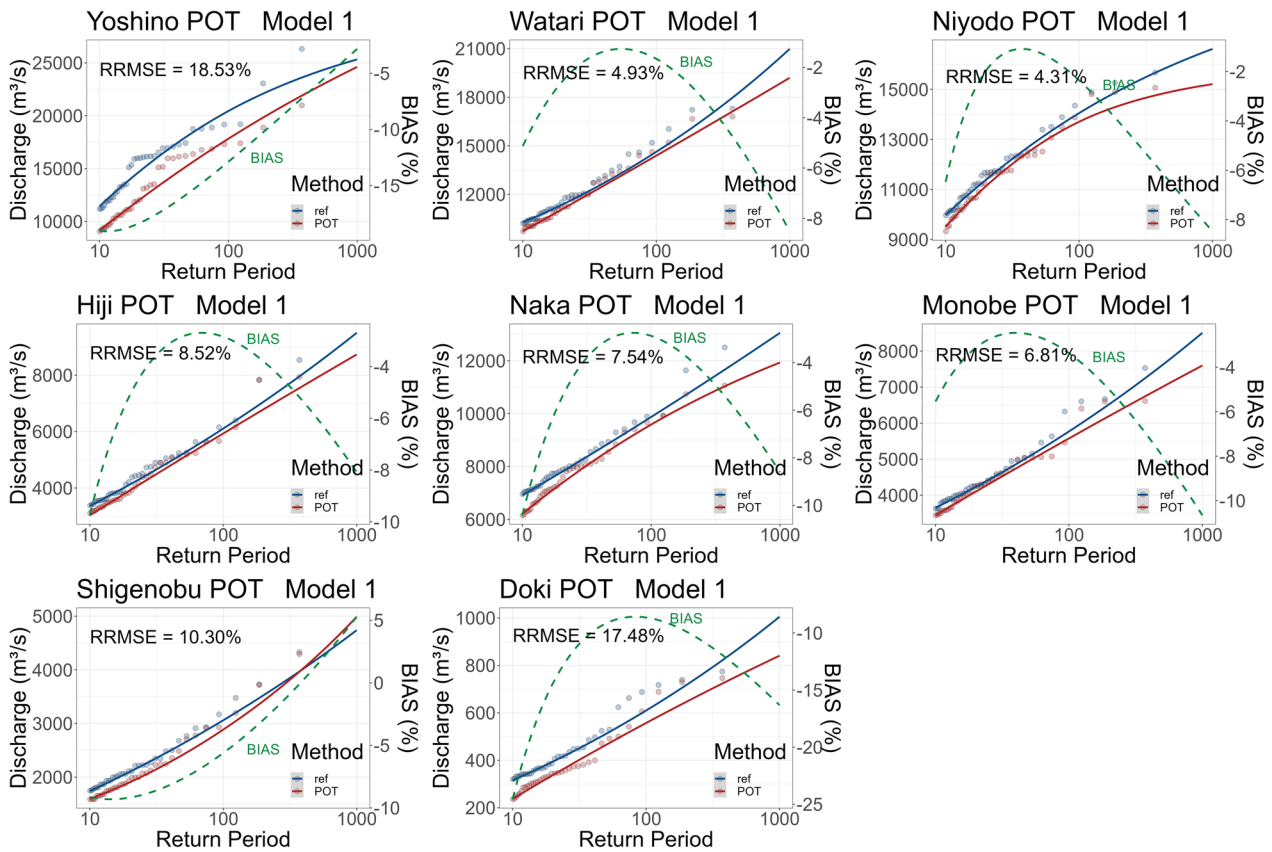


Fig. 7 Estimation results of discharge quantiles for different basins using the POT methods with the top 10% AMFS for the 4 K warming scenario

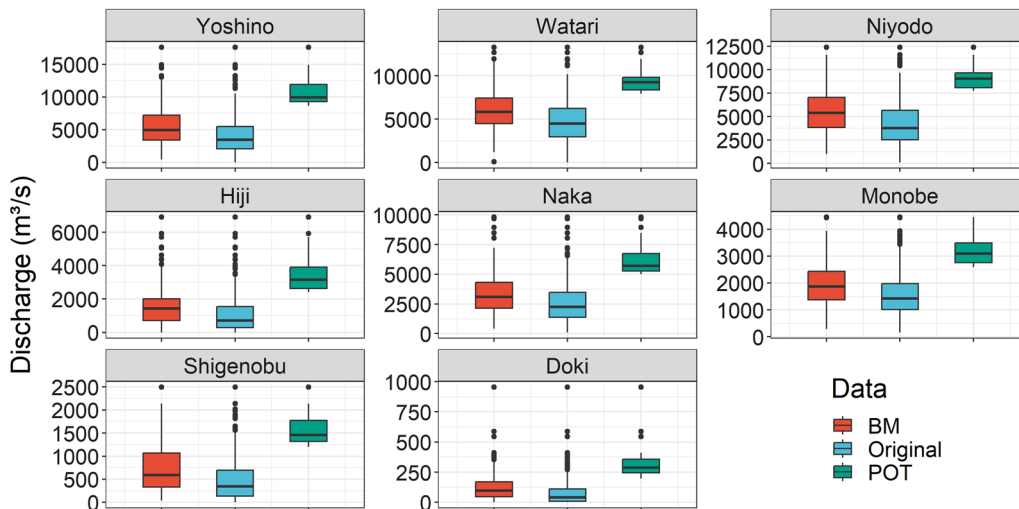


Fig. 8 Distribution of processed (POT and BM) and original regional AMFS with optimal selection parameters in the current scenario

future scenarios without a significant increase in error. This suggests that the regional approach is compatible with the potential changes in climatic conditions. Second,

the error underscores the pivotal role of local extreme precipitation events in future flood risk assessments, emphasizing the importance of utilizing detailed climate

projection ensembles. Recent studies on the dynamic downscaling of climate data have focused on convection-permitting models with higher resolution (National Institute for Environmental Studies 2022) because convection is a potential mechanism of extreme precipitation that varies with climate warming (Pendergrass 2020) and causes extremely severe precipitation (Qin et al. 2022).

To meet the emerging demand for handling high-resolution climate projection ensembles in flood research, developing event-based regional approach is crucial. Future studies should prioritize the reduction of the second type of error. A potential direction could be developing event extraction methods that independent from statistical indicators, keeping natural evolution of precipitation and capturing local extreme precipitation.

6 Conclusions

To fully leverage large climate projection ensembles and provide discharges at specific return periods for large-scale flood hazard maps with limited computing resources, this study proposes an event-based high-resolution simulation and analysis scheme called the regional approach. Using Shikoku Island and its eight major basins as an example, the applicability of this approach was verified using a 150 m resolution RRI model, and the sources of error were analyzed. This study contributes to the development of big data processing techniques in hydrology. The conclusions are as follows:

1. The top 10–50% of AMFS for the POT method are the reasonable combinations for the regional approach. The POT method is more recommended than the BM method.
2. Using the regional approach, the RRMSE of each basin was maintained within 20%. The main source of error was attributed to the fixed duration of 48 h being unable to fully cover the peak occurrence times of all basins. Moreover, using annual maximum 48 h rainfall as the extraction criterion may miss extreme precipitation events with short durations.
3. The regional approach designed in this study showed good accuracy under current, 2 K warming, and 4 K warming scenarios and can provide future flood quantiles consistent with those obtained from the basin approach.

Abbreviations

| | |
|----------|---|
| 48 h-AMS | 48 h annual maximum precipitation series |
| AMFS | Annual maximum flood series |
| BM | Block maxima |
| BIAS | Relative bias |
| d4PDF | Database for policy decision-making for future climate change |

| | |
|---------------|--|
| FFA | Flood frequency analysis |
| GPD | Generalized Pareto distribution |
| MRI-AGCM 3.2 | Meteorological Research Institute Atmospheric General Circulation Model 3.2 |
| NHRCM | Non-hydrostatic regional climate model |
| PE3 | Pearson type III |
| POT | Peak over threshold |
| RRI | Rainfall–runoff–inundation |
| RRMSE | Relative root-mean-square error |
| SI-CAT DDS5TK | Dynamical DownScaling data for near-future atmospheric projection (from Tohoku to Kyushu) by the Social Implementation program on Climate change Adaptation Technology |
| SST | Sea surface temperature |
| WEB-RRI | Water and energy budget-based RRI |

Supplementary Information

The online version contains supplementary material available at <https://doi.org/10.1186/s40645-024-00618-x>.

Additional file 1. Selection of the optimal distribution for block maxima method.

Acknowledgements

We acknowledge MLIT of Japan for providing hydrologic and river data. We acknowledge Assoc. Prof. Dai Yamazaki for providing J-FlwDir, which JRRI model uses for flow direction. We acknowledge Mr. Ayato Yamakita for the detailed validation of the model.

Author contributions

JC performed the data processing, analysis, and manuscript writing. TS proposed the topic, designed, and performed the simulations, and provided suggestions for this manuscript. MY and YS contributed to model development and suggestions to this manuscript. All the authors have read and approved the final version of the manuscript.

Funding

This work was supported by the MEXT Program for the Advanced Studies of Climate Change Projection (SENTAN) [Grant Number: JPMXD0722678534], Cabinet Office, Government of Japan, and Cross-Ministerial Strategic Innovation Promotion Program (SIP) (PI: Kusunoki). For the model development phase, this work was supported by collaborative research Grants provided by Kyoto Prefecture, Japan Society for the Promotion of Science (JSPS) KAKENHI [Grant JP19H02248 for PI: Sayama, JP21H04597 for PI: Yamori, and JP22H01600 for PI: Tachikawa].

Availability of data and materials

The simulation datasets created in this study are available from the corresponding author upon request.

Declarations

Ethical approval and consent to participate

Not applicable.

Consent for Publication

Not applicable.

Competing interest

The authors declare that they have no competing interest.

Received: 20 August 2023 Accepted: 15 March 2024

Published online: 25 March 2024

References

- Alfieri L, Salamon P, Bianchi A, Neal J, Bates P, Feyen L (2014) Advances in pan-European flood hazard mapping. *Hydrol Process* 28(13):4067–4077
- Bates PD, Horritt MS, Fewtrell TJ (2010) A simple inertial formulation of the shallow water equations for efficient two-dimensional flood inundation modelling. *J Hydrol* 387(1):33–45
- Beguéría S (2005) Uncertainties in partial duration series modelling of extremes related to the choice of the threshold value. *J Hydrol* 303(1):215–230
- Bezak N, Brilly M, Šraj M (2014) Comparison between the peaks-over-threshold method and the annual maximum method for flood frequency analysis. *Hydrol Sci J* 59(5):959–977
- Bhagabati SS, Kawasaki A (2017) Consideration of the rainfall-runoff-inundation (RRI) model for flood mapping in a deltaic area of Myanmar. *Hydrol Res Lett* 11(3):155–160
- Breini K, Lun D, Müller-Thomy H, Blöschl G (2021) Understanding the relationship between rainfall and flood probabilities through combined intensity-duration-frequency analysis. *J Hydrol* 602:126759
- Cash J, Karp A (1990) A variable order Runge–Kutta method for initial-value problems with rapidly varying right-hand sides. *Acm Trans Math Softw* 16(3):201–222
- Cunnane C (1973) A particular comparison of annual maxima and partial duration series methods of flood frequency prediction. *J Hydrol* 18(3):257–271
- Deushi M, Shibata K (2011) Development of a meteorological research institute chemistry-climate model version 2 for the study of tropospheric and stratospheric chemistry. *Pap Meteorol Geophys* 62:1–46
- Dottori F, Salamon P, Bianchi A, Alfieri L, Hirpa FA, Feyen L (2016) Development and evaluation of a framework for global flood hazard mapping. *Adv Water Resour* 94:87–102
- Ferreira A, de Haan L (2015) On the block maxima method in extreme value theory: PWM estimators. *Ann Stat* 43(1):276–298
- Fujita M, Mizuta R, Ishii M, Endo H, Sato T, Okada Y et al (2019) Precipitation changes in a climate with 2-K surface warming from large ensemble simulations using 60-km global and 20-km regional atmospheric models. *Geophys Res Lett* 46(11):435–442
- Gellens D (2002) Combining regional approach and data extension procedure for assessing GEV distribution of extreme precipitation in Belgium. *J Hydrol* 268(1):113–126
- Green WH, Ampt GA (1911) Studies on soil physics. *J Agric Sci* 4(1):1–24. <https://doi.org/10.1017/S0021859600001441>
- Hatsuzuka D, Sato T, Yoshida K, Ishii M, Mizuta R (2020) Regional projection of tropical-cyclone-induced extreme precipitation around Japan based on large ensemble simulations. *Sola* 16:23–29
- Hirabayashi Y, Mahendran R, Koirala S, Konoshima L, Yamazaki D, Watanabe S, Kim H, Kanai S (2013) Global flood risk under climate change. *Nat Clim Chang* 3(9):816–821
- Hoch JM, Trigg MA (2019) Advancing global flood hazard simulations by improving comparability, benchmarking, and integration of global flood models. *Environ Res Lett* 14(3):034001
- Hosking JRM, Wallis JR (1993) Some statistics useful in regional frequency analysis. *Water Resour Res* 29(2):271–281
- Institute of Hydrology (1999) Flood estimation handbook. Institute of Hydrology, Wallingford
- IPCC (2021) Climate Change 2021: the physical science basis. Contribution of working group I to the sixth assessment report of the intergovernmental panel on climate change. Cambridge University Press, Cambridge
- Ishii M, Mori N (2020) d4PDF: large-ensemble and high-resolution climate simulations for global warming risk assessment. *Prog Earth Planet Sci* 7(1):58
- National Institute for Environmental Studies (2022) Bias corrected climate scenarios over Japan based on NHRCM02 using monthly CDFDM Ishizaki N. <https://doi.org/10.17595/20220415.001-e.html>. Accessed 14 Feb 2023
- Kamahori H, Arakawa O (2018) Tropical cyclone induced precipitation over Japan using observational data. *Sola Tokyo Meteorol Soc Jpn* 14:165–169
- Kawase H, Imada Y, Tsuguti H, Nakaegawa T, Seino N, Murata A, Takayabu I (2020) The heavy rain event of July 2018 in Japan enhanced by historical warming. *Bull Am Meteorol Soc* 101(11):S109–S114
- Kawase H, Murata A, Mizuta R, Sasaki H, Nosaka M, Ishii M, Takayabu I (2016) Enhancement of heavy daily snowfall in central Japan due to global warming as projected by large ensemble of regional climate simulations. *Clim Chang* 139(2):265–278
- Lang M, Ouara T, Bobee B (1999) Towards operational guidelines for over-threshold modeling. *J Hydrol* 225(3–4):103–117
- Langousis A, Malamakis A, Puliga M, Deidda R (2016) Threshold detection for the generalized Pareto distribution: review of representative methods and application to the NOAA NCDC daily rainfall database. *Water Resour Res* 52(4):2659–2681
- Madsen H, Rasmussen PF, Rosbjerg D (1997) Comparison of annual maximum series and partial duration series methods for modeling extreme hydrologic events: 1. At-Site Modeling. *Water Resour Res* 33(4):747–757
- Martínez C, Sanchez A, Toloh B, Vojinovic Z (2018) Multi-objective evaluation of urban drainage networks using a 1D/2D flood inundation model. *Water Resour Manag* 32(13):4329–4343
- Meade RH, Rayol JM, Da Conceição SC, Natividade JRG (1991) Backwater effects in the Amazon River basin of Brazil. *Environ Geol Water Sci* 18(2):105–114
- Miyasaka T, Kawase H, Nakaegawa T, Imada Y, Takayabu I (2020) Future projections of heavy precipitation in Kanto and associated weather patterns using large ensemble high-resolution simulations. *Sola* 16:125–131
- Mizuta R, Murata A, Ishii M, Shiogama H, Hibino K, Mori N et al (2017) Over 5,000 years of ensemble future climate simulations by 60-km global and 20-km regional atmospheric models. *Bull Am Meteorol Soc* 98(7):1383–1398
- Mostofi Zadeh S, Durocher M, Burn DH, Ashkar F (2019) Pooled flood frequency analysis: a comparison based on peaks-over-threshold and annual maximum series. *Hydrol Sci J* 64(2):121–136
- Ohba M, Arai R, Toyoda Y, Sato T (2022) Impact of weather regime on projected future changes in streamflow in a heavy snowfall area of Japan. *Clim Dyn* 59(3):939–950
- Ohba M, Sugimoto S (2019) Differences in climate change impacts between weather patterns: possible effects on spatial heterogeneous changes in future extreme rainfall. *Clim Dyn* 52(7):4177–4191
- Otaki T, Fudeyasu H, Kohno N, Takemi T, Mori N, Iida K (2022) Investigation of characteristics of maximum storm surges in Japanese coastal regions caused by typhoon Jebi (2018) based on typhoon track ensemble simulations. *J Meteorol Soc Jpn* 100(4):661–676
- Packman JC, Kidd CHR (1980) A logical approach to the design storm concept. *Water Resour Res* 16(6):994–1000
- Pappenberger F, Dutra E, Wetterhall F, Cloke HL (2012) Deriving global flood hazard maps of fluvial floods through a physical model cascade. *Hydrol Earth Syst Sci* 16(11):4143–4156
- Pendergrass AG (2020) Changing degree of convective organization as a mechanism for dynamic changes in extreme precipitation. *Curr Clim Chang Rep* 6(2):47–54
- Qin H, Yuan W, Wang J, Chen Y, Dai P, Sobel AH, Meng Z, Nie J (2022) Climate change attribution of the 2021 Henan extreme precipitation: impacts of convective organization. *Sci China Earth Sci* 65(10):1837–1846
- Rasmy M, Sayama T, Koike T (2019) Development of water and energy budget-based rainfall-runoff-inundation model (WEB-RR) and its verification in the Kalu and Mundeni River Basins, Sri Lanka. *J Hydrol* 579:124163
- Sampson CC, Smith AM, Bates PD, Neal JC, Alfieri L, Freer JE (2015) A high-resolution global flood hazard model. *Water Resour Res* 51(9):7358–7381
- dos Santos CM, Escobedo JF, Teramoto ET, da Silva SHMG (2016) Assessment of ANN and SVM models for estimating normal direct irradiation (Hb). *Energy Convers Manag* 126:826–836
- Sasai T, Kawase H, Kanno Y, Yamaguchi J, Sugimoto S, Yamazaki T, Sasaki H, Fujita M, Iwasaki T (2019) Future projection of extreme heavy snowfall events with a 5-km large ensemble regional climate simulation. *J Geophys Res Atmos* 124(24):13975–13990
- Sasaki H, Murata A, Hanafusa M, Ohizumi M, Kurihara K. (2011) Reproducibility of present climate in a non-hydrostatic regional climate model nested within an atmosphere general circulation model. *Sola* 7:173–176
- Sayama T, McDonnell JJ (2009) A new time-space accounting scheme to predict stream water residence time and hydrograph source components at the watershed scale. *Water Resour Res* 45:W07401
- Sayama T, Ozawa G, Kawakami T, Nabesaka S, Fukami K (2012) Rainfall-runoff-inundation analysis of the 2010 Pakistan flood in the Kabul River basin. *Hydrol Sci J* 57(2):298–312
- Sayama T, Tatebe Y, Iwami Y, Tanaka S (2015) Hydrologic sensitivity of flood runoff and inundation: 2011 Thailand floods in the Chao Phraya River basin. *Nat Hazards Earth Syst Sci* 15(7):1617–1630

- Sayama T, Tatebe Y, Tanaka S (2017) An emergency response-type rainfall-runoff-inundation simulation for 2011 Thailand floods. *J Flood Risk Manag* 10(1):65–78
- Sayama T, Yamada M, Sugawara Y, Yamazaki D (2020) Ensemble flash flood predictions using a high-resolution nationwide distributed rainfall-runoff model: case study of the heavy rain event of July 2018 and Typhoon Hagibis in 2019. *Prog Earth Planet Sci* 7(1):75
- Smith A, Sampson C, Bates P (2015) Regional flood frequency analysis at the global scale. *Water Resour Res* 51(1):539–553
- Sun Y, Wendi D, Kim DE, Liong S-Y (2019) Deriving intensity–duration–frequency (IDF) curves using downscaled in situ rainfall assimilated with remote sensing data. *Geosci Lett* 6(1):17
- Swetapadma S, Ojha CSP (2021) Technical note: flood frequency study using partial duration series coupled with entropy principle. *Hydrol Earth Syst Sci* 2021:1–23
- Tada H, Uchiyama Y, Masunaga E (2018) Impacts of two super typhoons on the Kuroshio and marginal seas on the Pacific coast of Japan. *Deep-Sea Res Part I* 132:80–93
- Tanaka T, Tachikawa Y, Ichikawa Y, Yorozu K (2018) Flood risk curve development with probabilistic rainfall modelling and large ensemble climate simulation data: a case study for the Yodo River basin. *Hydrol Res Lett* 12(4):28–33
- Tellman B, Sullivan JA, Kuhn C, Kettner AJ, Doyle CS, Brakenridge GR, Erickson TA, Slayback DA (2021) Satellite imaging reveals increased proportion of population exposed to floods. *Nature* 596(7870):80–86
- Try S, Tanaka S, Tanaka K, Sayama T, Khujanazarov T, Oeurng C (2022) Comparison of CMIP5 and CMIP6 GCM performance for flood projections in the Mekong River Basin. *J Hydrol Reg Stud* 40:101035
- Wasko C, Nathan R, Stein L, O’Shea D (2021) Evidence of shorter more extreme rainfalls and increased flood variability under climate change. *J Hydrol* 603:126994
- Watt E, Marsalek J (2013) Critical review of the evolution of the design storm event concept. *Can J Civ Eng* 40(2):105–113
- Wing OEJ, Bates PD, Sampson CC, Smith AM, Johnson KA, Erickson TA (2017) Validation of a 30 m resolution flood hazard model of the conterminous United States. *Water Resour Res* 53(9):7968–7986
- Wing OEJ, Smith AM, Marston ML, Porter JR, Amodeo MF, Sampson CC, Bates PD (2021) Simulating historical flood events at the continental scale: observational validation of a large-scale hydrodynamic model. *Nat Hazards Earth Syst Sci* 21:559–575
- Winsemius HC, Jongman B, Veldkamp TIE, Hallegatte S, Bangalore M, Ward PJ (2018) Disaster risk, climate change, and poverty: assessing the global exposure of poor people to floods and droughts. *Environ Dev Econ* 23(3):328–348
- Winsemius HC, Van Beek LPH, Jongman B, Ward PJ, Bouwman A (2013) A framework for global river flood risk assessments. *Hydrol Earth Syst Sci* 17(5):1871–1892
- Yamada M, Sayama T, Yamazaki D, Watanabe M (2022) Development of methodology for introducing surveyed river cross-sections into nationwide distributed hydrological model throughout Japan, and its effect on water level prediction accuracy. *J Jpn Soc Civ Eng Ser B Hydraul Eng* 78(1):7–22
- Yamakita A (2023) Parameter regionalization of a nationwide hydrologic model and its validation at multiple locations. Dissertation, Kyoto University
- Yamamoto K, Sayama T, Apip (2021) Impact of climate change on flood inundation in a tropical river basin in Indonesia. *Prog Earth Planet Sci* 8(1):5
- Yamazaki D, de Almeida GAM, Bates PD (2013) Improving computational efficiency in global river models by implementing the local inertial flow equation and a vector-based river network map. *Water Resour Res* 49(1):7221–7235
- Yan Z, Xia J, Song J, Zhao L, Pang G (2020) Research progress on design hydrographs in small and medium-scale basins. *Prog Geogr* 39(7):1224–1235
- Yao HX, Creed IF (2005) Determining spatially-distributed annual water balances for ungauged locations on Shikoku Island, Japan: a comparison of two interpolators. *Hydrol Sci J* 50(2):245–263
- Yoshida R, Iizumi T, Nishimori M, Yokozawa M (2012) Impacts of land-use changes on surface warming rates and rice yield in Shikoku, western Japan. *Geophys Res Lett* 39:L22401
- Yukimoto S, Adachi Y, Hosaka M, Sakami T, Yoshimura H, Hirabara M, Tanaka T, Shindo E, Tsujino H, Deushi M, Mizuta R, Yabu S, Obata A, Nakano H, Koshiro T, Ose T, Kitoh A (2012) A new global climate model of the meteorological research institute: MRI-CGCM3—Model description and basic performance. *J Meteorol Soc Jpn Ser II* 90A:23–64
- Zeng Z, Wang Z, Lai C (2022) Simulation performance evaluation and uncertainty analysis on a coupled inundation model combining SWMM and WCA2D. *Int J Disaster Risk Sci* 13(3):448–464
- Zhao F, Veldkamp TIE, Frieler K, Schewe J, Ostberg S, Willner S, Schauburger B, Gosling SN, Schmied HM, Portmann FT, Leng G, Huang M, Liu X, Tang Q, Hanasaki N, Biemans H, Gerten D, Satoh Y, Pokhrel Y, Stacke T, Ciais P, Chang J, Ducharme A, Guimberteau M, Wada Y, Kim H, Yamazaki D (2017) The critical role of the routing scheme in simulating peak river discharge in global hydrological models. *Environ Res Lett* 12(7):075003
- Zou N, Volgushev S, Buecher A (2021) Multiple block sizes and overlapping blocks for multivariate time series extremes. *Ann Stat* 49(1):295–320

Publisher’s Note

Springer Nature remains neutral with regard to jurisdictional claims in published maps and institutional affiliations.